DOI: 10.1002/ejoc.201000215

Off the Back or on the Side: Comparison of *meso* and 2-Substituted Donor-Acceptor Difluoroborondipyrromethene (Bodipy) Dyads

Andrew C. Benniston,*[a] Graeme Copley,[a] Helge Lemmetyinen,*[b] and Nikolai V. Tkachenko[b]

Keywords: Dyes / Luminescence / Fluorescence / Electrochemistry / Photochemistry / Electron transfer

The preparation of several difluoroborondipyrromethene (Bodipy) dyads is described incorporating covalently attached hydroquinone/quinone groups at the 2-position (**BD-SHQ**, **BD-SQ**, **BD-SPHQ**, **BD-SPQ**). The compounds, currently under investigation as chemical sensors for reactive oxygen species, show various levels of fluorescence depending on the oxidation state of the appended group. The ^{19}F NMR spectrum for **BD-SHQ** in $CDCl_3$ at room temperature reveals the two fluorines are inequivalent on the NMR timescale. In contrast, the ^{19}F NMR spectrum for the counterpart quinone compound, **BD-SQ**, is consistent with two equivalent fluorine atoms. The two results are interpreted as the quinone is free to rotate around the connector bond, whereas this motion is restricted for the hydroquinone group and makes the fluorines chemically inequivalent. Cyclic voltammograms recorded for all derivatives in CH_2Cl_2 electrolyte solution are consistent with typical Bodipy-based redox chemistry; the potentials of which depend on factors such as presence of the phenylene spacer and oxidation state of the appended group. A comparison of the electrochemical behaviour with the counterpart *meso* derivatives reveals some interesting trends which are associated with the location of the HOMO/LUMOs. The absorption profiles for the compounds in CH_3CN are again consistent with Bodipy-based derivatives, though there are some subtle differences in the band-shapes of the closely-coupled systems. In particular, the absorption spectra for the dyad, **BD-SQ**, in a wide range of solvents are appreciably broader than for **BD-SHQ**. Femtosecond transient absorption spectroscopy performed on the hydroquinone derivatives, **BD-SHQ** and its *meso* analogue is interpreted as electron transfer occurs from the hydroquinone unit to the first-excited singlet (S_1) state of the Bodipy center, followed by ultrafast charge recombination to reinstate the ground state. The coupling of OH vibrations to the return electron transfer process is invoked to explain the lack of clear identification of the charge-separated state in the transient records.

Introduction

In the search for new and more robust fluorescent dyes one type of molecular system is certainly emerging as a serious frontrunner: the half-porphyrin dye, difluoroborondipyrromethene (Bodipy).[1] The rise in popularity in the dye can be certainly traced to its highly beneficial traits such as high fluorescence yield, high molar absorption coefficient, good photostability, readily tunable absorption profile and excellent excited-state redox behaviour.[2] Like many other researches we have focussed on the latter point and how this can be used in the development of molecular probes[3] that respond to outside influences such as pH,[4] metal ions,[5] gases,[6] and radicals.[7] The detection of reactive oxygen species (ROS) in biological specimens is one area that current resources are being put into considering the extreme importance of ROS in many biologically important processes.[8] Previously we described the response of the *meso* hydroquione derivatives, **BD-MPHQ** (Figure 1), to hydrogen peroxide in a membrane mimic.[9] The derivative **BD-MPHQ** behaves as an excellent fluorescence-by-eye detector of hydrogen peroxide, and has the added benefit of being reversible since the quinone derivative (**BD-MPQ**) can be reduced back in situ to the active probe. In seeking new probes we developed the analogue series in which the ROS sensitive group is appended in the 2-position. One intention was to see if the on/off discrimination level could be improved by a change in substitution pattern. Here we discuss the comparison of the two series highlighting in particular differences in their electrochemical and photophysical behaviour.

[a] Molecular Photonics Laboratory, School of Chemistry, Newcastle University,
Newcastle upon Tyne, NE1 7RU, UK
Fax: +44-191-222-6929
E-mail: a.c.benniston@ncl.ac.uk
[b] The Department of Chemistry and Bioengineering, Tampere University of Technology,
P. O. Box 541, 33101, Finland
Supporting information for this article is available on the WWW under http://dx.doi.org/10.1002/ejoc.201000215.

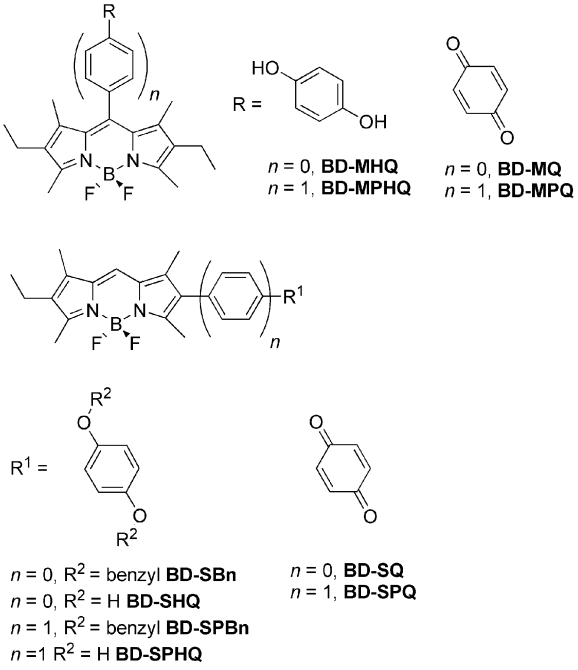

Figure 1. The Bodipy compounds discussed in the text and their basic nomenclature.

Results and Discussion

Synthesis

In devising a synthetic procedure towards the 2-substituted Bodipy analogues our main aim was to prepare mono-substituted derivatives only, even though symmetrical versions may have been more easier to produce since a literature procedure was at hand for preparing 2,6-dibromo/iodo Bodipy derivatives.[10] The outlined method shown in Scheme 1 towards the target molecules represents the most successful approach, utilizing optimized protecting groups (Boc and Bn) and having the protected quinone in place from the start of the synthesis.[11] Other protecting groups for the hydroxy groups (e.g., TIPS) were tried but failed to survive the full synthetic procedure. The starting building block is compound **1**, which is readily prepared in three steps using reported literature procedures.[12] Compound **2a** is an easily prepared precursor starting from 2-bromobenzene-1,4-diol in two steps. To prepare the analogue compound, **2b**, a literature procedure[13] was slightly adapted in which 4-bromoaniline is firstly converted to 4′-bromobiphenyl-2,5-diol, then protected with the benzyl groups and finally converted into the boronic acid. Cross coupling of **2a/2b** with **1** using standard Suzuki conditions[14] produced the substituted pyrrole derivatives **3a/3b** in good yields. The next step and formation of the Bodipy core followed the standard literature procedure[1a] of condensation of **3a/3b** with 3-ethyl-2,4-dimethylpyrrole in the presence of base, coupled with oxidation and chelation to the difluoroboron group. Both the protected compounds, **BD-SBn** and **BD-SPBn**, were purified extensively by column chromatography to afford dark violet solids. The first attempted method for removal of the benzyl protecting group under one atmosphere of H_2 in the presence of Pd/C failed to yield the desired compounds. Instead, both the compounds decomposed to dipyrromethane side products due to hydrogenation of the unmasked *meso* double bond.[1b] Use of the milder condition of 1,4-cyclohexadiene and $Pd(OH)_2/C$, however, was more successful and gave the hydroquinone compounds, **BD-SHQ** and **BD-SPHQ**, in excellent yields. Oxidation of the hydroquinone group to the quinone moiety performed using DDQ worked extremely well to afford **BD-SQ** and **BD-SPQ** in good yields after careful chromatography. For all spectroscopic work the quinone compounds were also purified by preparative tlc (silica gel, CH_2Cl_2) to remove trace amounts of the hydroquinone compounds. All compounds were fully characterized by numerous analytical techniques including ^1H, ^{13}C, ^{11}B and ^{19}F NMR spectroscopy, mass spectrometry and elemental

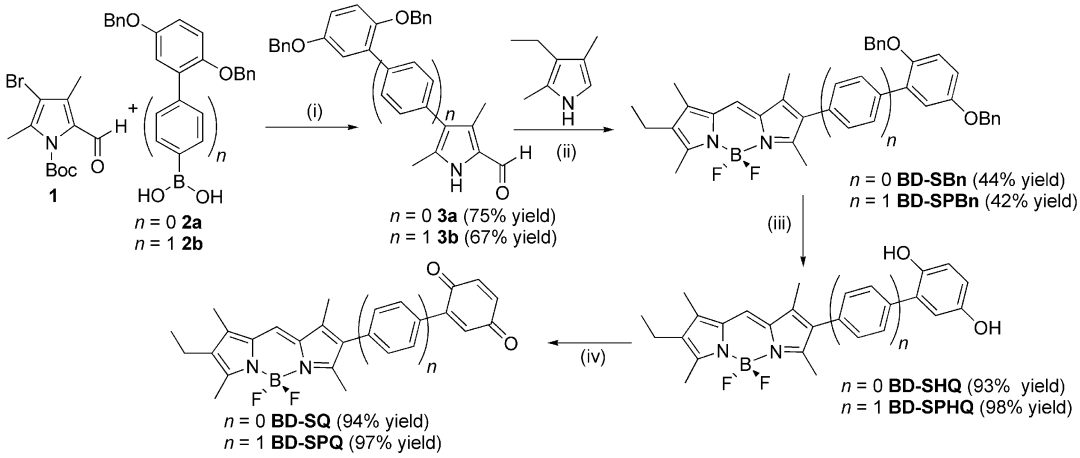

Scheme 1. Reagents and conditions. (i) DMF, Na_2CO_3, $Pd(PPh_3)_4$, reflux. (ii) CH_2Cl_2, TFA, *N*,*N*-diisopropylethylamine, $BF_3{\cdot}Et_2O$, room temperature, (iii) EtOH, 1,4-cyclohexadiene, $Pd(OH)_2/C$, reflux (iv) THF, DDQ.

analysis. Single-crystal structural analysis was performed on several compounds, including **BD-SBn**, **BD-SPBn** and **BD-SPQ**, and confirmed their identity.[15]

^{19}F NMR Spectroscopy

Previous findings have shown that ^{19}F chemical shifts for Bodipy derivatives can be highly sensitive to the local environment.[9,16] For example, the two fluorines in **BD-MQ** are inequivalent on the NMR time scale owing to restricted rotation of the quinone group which is caused by the two 1,7-methyl groups. Inspection of a simple space-filling model generated from the crystal structure determination of **BD-SBn** reveals that the 1–3 dimethyl groups will restrict rotation of the appended aromatic group. This notion was in fact borne out in the room temperature ^{19}F NMR spectrum for the compound which shows 14 lines. The spectrum is adequately simulated as two chemically inequivalent fluorines ($\Delta\delta$ = 0.43 ppm) coupling ($^{Fa–Fb}J$ = 107 Hz) to the quadropolar ^{11}B nuclei ($^{B–F}J$ = 35 and 34 Hz) (see Supporting Information). A somewhat similar looking ^{19}F spectrum (12 lines) is seen for **BD-SHQ** (Figure 2), but in this case the difference in chemical shift between the two fluorines is smaller ($\Delta\delta$ = 0.29 ppm) (see Supporting Information). To account for these two observations the aromatic group must undergo, at least on the NMR timescale, restricted rotation so that each fluorine is in a different chemical environment. In contrast to these two cases, the ^{19}F NMR spectrum for **BD-SQ** is very simple and contains a quartet with signs of smaller secondary coupling. The spectrum is simulated as two equivalent fluorines coupling to the ^{11}B (I = 3/2, 80.42%) and ^{10}B (I = 3, 19.58%) nuclei. It would appear that the small change in molar volume (ca. 9 cm^3 mol^{-1})[17] in shifting from hydroquinone to quinone is enough to permit rotation around the connector bond. At a basic level

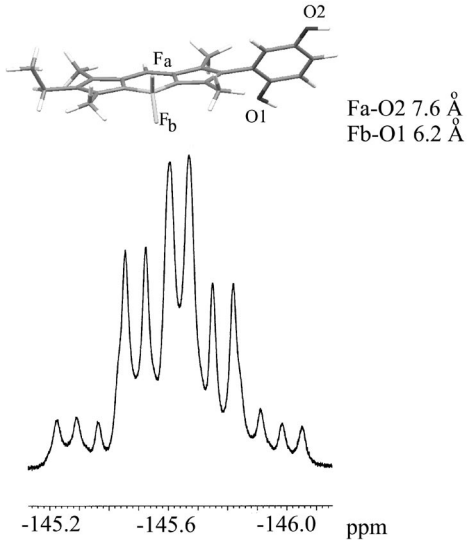

Figure 2. The room temperature ^{19}F NMR (470 MHz) spectrum for **BD-SHQ** in $CDCl_3$, and a basic molecular model showing the proximity of the oxygen atoms to the fluorine atoms.

the compound **BD-SQ** can be considered a redox molecular brake,[18] since free rotation is retarded upon reduction to the hydroquinone, and reversed upon oxidation back to the quinone. This idea was not followed up further, but it was noted that **BD-SHQ** (and any derivative thereof) is chiral at the boron centre since the Bodipy core is asymmetrical and the two fluorines are inequivalent. No attempt was made to try and isolate the two chiral rotamers, but in principle this may be possible by attaching chiral group(s) to the hydroxys to produce diasteroisomers.[19]

Electrochemistry

The electrochemical behavior of the Bodipy derivatives was measured by the standard cyclic voltammetry (CV) technique in dry CH_2Cl_2 containing 0.2 M *N*-tetrabutylammonium tetrafluoroborate (TBATFB) electrolyte at a platinum electrode. The redox half-wave potentials ($E_{1/2}$) are quoted relative to the ferrocenium/ferrocene couple which is taken to be fully reversible, and peak separations ($E_{pa} - E_{pc}$) for other redox couples are compared to that observed for ferrocene (60 mV as measured). Very clean looking CVs were recorded in most of the cases for the Bodipy derivatives, and there was no appreciable sign of electrode fouling under the employed conditions. The quinone derivatives, **BD-SQ** and **BD-SPQ**, display upon reductive scanning a clear quasi-reversible one-electron wave at around –0.90 V (peak separation ≈ 160 mV) that is assigned to the redox processes associated with the quinone group (see Supporting Information). At a considerable more cathodic potential the one electron reduction of the Bodipy moiety is observed, which for **BD-SPQ** is completely irreversible. The redox process at the Bodipy site is clearly perturbed by the presence of the quinone radical anion. The oxidative portion of the CV is dominated by a quasi-reversible wave at around +0.75 V (peak separation ≈ 100 mV), that is readily assigned, by comparison to literature examples,[20] to one-electron oxidation of the Bodipy core.

The CVs. of the dihydroxy (**BD-SHQ/BD-SPHQ**) and benzyl-protected derivatives (**BD-SBn/BD-SPBn**) again, in the reductive segment of the CV, show the characteristic wave associated with one-electron reduction of the Bodipy unit. The oxidative portion contains two waves with one being assigned to the one-electron oxidation of the Bodipy unit and the second to oxidation of the hydroquinone or benzyloxy group. Electrochemical data for all the compounds, and that previously published for the *meso* derivatives,[9] are collected in Table 1. In comparing the redox potentials for the 2-substituted Bodipy compounds, as well as the *meso* counterparts, several interesting trends are revealed, including effects of adding the phenylene spacer, change from hydroquinone to quinone and alteration in substitution position. In attempting to rationalize the electrochemical results several, often competing factors need to be taken into account including, for example, effects from change in the extent of π-conjugation (steric induced), alteration in electron donor/acceptor ability of appended group,

adjustment in charge distribution in the molecular framework and change in spatial arrangement of the HOMO/LUMOs on the Bodipy core. In addition, considering that quinone is a good electron acceptor a strongly-coupled polarization in the ground-state molecule might be expected along the line $BD^{\delta+}$-$Q^{\delta-}$, and would make oxidation more difficult. This argument would also hold for the hydroquinone which is more of an electron donor and the polarization would be $BD^{\delta-}$-$HQ^{\delta+}$ and make oxidation easier. Electronic coupling would be enhanced by increased conjugation along the molecular framework. The aryl spacer group could act to either decouple/couple the two subunits.

Table 1. Electrochemical data for the Bodipy compounds discussed in the text.

Compd.	E^1 /V[a]	E^2 /V[b]	E^3 /V[c]	E^4 /V[d]	ΔE^1 /V[e]	ΔE^2 /V[f]
BD-SBn	0.61	–1.70	–	1.10	2.31	0.49
BD-SPBn	0.64	–1.64	–	0.97	2.28	0.33
BD-SHQ	0.76	–1.62	–	0.53	2.38	0.23
BD-SPHQ	0.67	–1.58	–	0.58[g]	2.25	[h]
BD-SQ	0.75	–1.56	–0.91	–	2.31	0.65
BD-SPQ	0.66	–1.46[g]	–0.87	–	2.12	[h]
BD-MHQ	0.82	–1.58	–	0.61	2.40	0.21
BD-MPHQ	0.76[g]	–1.50	–	0.56[g]	2.26	[h]
BD-MQ	0.71	–1.81	–0.79	–	2.52	1.02
BD-MPQ	0.63	–1.79	–0.90	–	2.42	0.89

[a] $E_{1/2}$ for one-electron oxidation of Bodipy. [b] $E_{1/2}$ for one-electron reduction of Bodipy. [c] $E_{1/2}$ for one-electron reduction of quinone. [d] $E_{1/2}$ for one-electron oxidation of hyroquinone/benzyloxy. [e] $E^1 - E^2$. [f] Modulus of $E^4 - E^1$ or $E^2 - E^3$. [g] No reverse peak observed. [h] Not calculated because of irreversibility of redox process.

The affect of the phenylene group is clearly seen by comparing oxidation potentials and, to a lesser extent, the reduction potentials for the hydroquinone/quinone derivatives for both the series. Ignoring redox potentials obtained from CVs that are not fully reversible, then phenylene insertion leads to a definite shift to a less positive potential (ca. –90 mV) for oxidation of the Bodipy core, and arguably a small anodic shift in the Bodipy reduction potential. It is noticeable that ΔE^1 ($E^1 - E^2$) which represents the HOMO–LUMO gap is reduced by insertion of the aryl spacer. An increase in π-conjugation (raising of the HOMO) is consistent with the first observation but not the second since the LUMO would be lowered in energy and make the Bodipy center harder to reduce. Presumably a secondary electronic effect perturbs the LUMO. The quinone-based redox potentials for **BD-SQ**, **BD-SPQ** and **BD-MPQ** are very similar and appreciably more cathodic than the redox potential for **BD-MQ**. It is clear that no real ground-state polarization dominates since reduction would be expected to be the more difficult for the directly-linked quinone derivatives. Additionally, any effect from extended conjugation of the quinone with the Bodipy core seems inconsistent with the lack of difference between **BD-SQ** and **BD-SPQ**. The similar redox potentials for **BD-SQ** and **BD-MPQ** are also in line with this argument, since in the latter derivative the two methyl groups restrict any extended π-conjugation. It appears that the reduction potential for **BD-MQ** is the odd one out. The comparison of the oxidation potentials for the hydroquinone group is difficult because of the irreversibility of the redox couple for the two phenylene spacer derivatives. However, oxidation of the hydroquinone group in **BD-MHQ** is slightly more difficult than for **BD-SHQ**. This is, as expected, the opposite of what is observed in the quinone reduction potentials. It is worth noting that the change from hydroquinone to quinone has very little affect on the Bodipy-based oxidation potentials (E^1) for the 2-substituted Bodipy derivatives, and only affects slightly the reduction potentials where the shift is anodic (+ 60 mV). In contrast, alteration in oxidation potentials for the *meso*-substituted Bodipy derivatives is significant and cathodic (–110 mV), and coupled to a concomitant shift to a more cathodic potential (–230 mV) for the Bodipy-based reduction. These findings suggest that the Bodipy-based LUMO and HOMO for the *meso* derivatives are highly perturbed by a change in oxidation state of the appended group, but any change for the 2-substituted derivatives is much less pronounced.

A small shift to a lower potential (–40 mV) is observed for the Bodipy-based oxidation when a comparison is made between **BD-SQ** and **BD-MQ**. For the hydroquinone derivatives, **BD-SHQ** and **BD-MHQ**, the change in substitution pattern results in an anodic shift (+ 60 mV). Again, for the directly linked derivatives, there is a noticeable cathodic shift (–250 mV) in the Bodipy-based reduction potentials by modification of the substitution pattern from side-on to the *meso* position. This is less evident in the hydroquinone case where in fact the shift (+ 40 mV) is to a higher reduction potential. What is apparent from Table 1 is that the peak separation between redox potentials for the quinone reduction and Bodipy reduction (ΔE^2) is much smaller for **BD-SQ** when compared to **BD-MQ**. The values for ΔE^2 when comparing the oxidation potentials associated with the hydroquinone oxidation and Bodipy oxidation are very similar and small. The magnitude of ΔE^2 affords direct information on the spatial location of charge on the Bodipy core and the quinone/hydroquinone groups. A large ΔE^2 indicates a close confinement of charge as observed for **BD-MQ**, which is consistent with the reduction in ΔE^2 by phenylene insertion (cf. **BD-MPQ**).

The smaller the separation the more remote are the opposite charges as seen in the case of **BD-SQ**. The location of the LUMO on the distal pyrrol ring in **BD-SQ** is in fitting with this idea, so as to maximize its separation from the singly-occupied molecular orbital (SOMO) on the quinone radical anion. The asymmetry of **BD-SQ** facilitates this process especially if the SOMO can mix with orbitals on the proximal pyrrol ring to bring the quinone radical anion into conjugation. In the symmetrical, **BD-MQ**, the SOMO cannot come into extended conjugation because of steric constraints. Previously published molecular orbital calculations performed on Bodipy derivatives[21] reveal that the HOMO state is mainly localized on the pyrrol units, with the LUMO spread over the backbone but with considerable electron density at the central *meso* atom. This

latter finding is consistent with the fact that addition of an electron to the LUMO is harder for **BD-MQ** because of the proximity of the SOMO on the quinone radical anion.

Absorption and Fluorescence Spectroscopy

Absorption and fluorescence spectra were recorded for the 2-substituted Bodipy compounds in dilute CH_3CN solution at room temperature. Data are collected in Table S2 (see Supporting Information) for all the compounds along with that for the *meso* derivatives. To aid in understanding the basic photophysical properties of the series, the starting materials **BD-SBn** and **BD-SPBn** were studied, and the findings discussed firstly for comparison purposes. The absorption spectrum for the benzyl protected compound **BD-SBn** is dominated by the typical Bodipy-like absorption profile at λ_{abs} = 525 nm, corresponding to the S_0–S_1 electronic transition.[1] The less intense band seen at around 382 nm is associated with the S_0–S_2 transition. The longer wavelength absorption profile for **BD-SBn** is somewhat broader and does not show the pronounced higher-energy shoulder observed for the counterpart *meso*-substituted derivative. This finding is in fitting with the overall reduction in symmetry of the molecule by the 2-substitution which perturbs the S_0 and S_1 states. A similar finding has been reported by Burgess et al.[22] for 2-substituted Bodipy-anthracene cassettes. Fluorescence is readily detected for **BD-SBn** and is centered at λ_{flu} = 549 nm, corresponding to a measured quantum yield of fluorescence (ϕ_{flu}) of 0.045. The fluorescence lifetime (τ_s) as determined by the single-photon-counting method is 300 ps. The radiative rate constant ($k_{RAD} = \phi_{flu}/\tau_s$) of 1.5×10^8 s^{-1} is typical for Bodipy-based dyes and similar to the value calculated using the Strickler–Berg expression.[23] The Stokes' shift of 833 cm^{-1} is somewhat larger than the value found for the *meso* derivative (499 cm^{-1}), which implies a more substantial alteration in molecular geometry takes place following the S_0–S_1 electronic transition and relaxation. It is more noticeable that non-radiative deactivation of the **BD-SBn** S_1 state is far more efficient than in **BD-MBn**, since the non-radiative rate constant (k_{NR}) is two orders of magnitude greater. The basic photophysical properties of the Bodipy group are noticeably affected by insertion of the phenylene group (cf. **BD-SPBn**). The absorption profile for **BD-SPBn** is similar in overall appearance, but slightly broadened and red-shifted, when compared to **BD-SBn**. A slight broadening of the fluorescence profile is also observed, and more importantly is accompanied by a significant increase in the Stokes' shift. These findings support increased conjugation of the phenylene group with the Bodipy unit in the S_1 excited state. Both the ϕ_{flu} and τ_s values for **BD-SPBn** are appreciably increased compared to **BD-SBn**. Clearly, the non-radiative decay process (Table S2, see Supporting Information) is curtailed by the insertion of the phenylene group. Reductive electron transfer quenching of the first-excited singlet state by the dibenzyloxyphenylene group in **BD-SBn** and **BD-SPBn** can be ruled out on thermodynamic grounds (see Supporting Information). It has been suggested that internal conversion in Bodipy dyes is affected by the flexibility, and extent of distortion from planarity, of the dipyrromethene backbone.[24] This is possibly one contribution coupled to the reduction of k_{NR} as predicted by the energy-gap law.[25]

The removal of the protecting groups to produce the hydroquinone derivatives **BD-SHQ** and **BD-SPHQ** does not bring about any major alterations in the absorption spectra for the two compounds. Fluorescence is still readily observed from **BD-SPHQ** with an emission profile that is very similar in appearance to **BD-SPBn**; the magnitude of the Stokes' shift is also very similar. The values for ϕ_{flu} and τ_s are, however, greatly reduced indicating the introduction of an additional first-excited singlet state deactivation process. Fluorescence quenching of the first-excited singlet state for **BD-SHQ** is more pronounced, and τ_s as measured by up-conversion spectroscopy is in the sub-picosecond region. It is very noticeable that τ_s for **BD-SPHQ** is reduced significantly ($\approx$ 25 fold) when compared to its complement *meso* derivative **BD-MPHQ**.

The most interesting findings relate to the major change in the absorption profile for the quinone derivative **BD-SQ** (Figure 3). The absorption profile in CH_3CN is noticeably broad (λ_{ABS} = 519 nm) with a very obvious lower-energy tail stretching off to around 700 nm. A Beer–Lambert plot (see Supporting Information) shows no deviation from linearity over the concentration range 2×10^{-5} M to 6.0×10^{-6} M, which rules out broadening caused by dye aggregation or intermolecular exciton coupling.[26] Absorption spectra recorded in a range of solvents show several interesting effects. In toluene, for example, the λ_{ABS} is red shifted by ca. 6 nm (cf. CH_3CN), and the absorption profile is considerably broader. Changing the solvent from toluene to MeTHF and finally formamide results in a blue-shift in λ_{ABS} and a narrowing of the absorption profile (Figure 3). This blue-shift is also observed for many other Bodipy derivatives[27] and in specific cases can be related to the solvent polarizability function [$f(n^2) = (n^2-1)/(2n^2+1)$]. To see if this was the case here, absorption spectra were recorded for **BD-SQ** in solvents of different polarizability for which it was soluble. Unfortunately, there is no clear connection between λ_{ABS} and $f(n^2)$ for the limited range of solvents used. The assignment of the lower-energy tail in the absorption spectrum to an intramolecular Bodipy-to-quinone optical charge-transfer (CT) band can be likely ruled out on the grounds that in polar solvents (i.e., CH_3CN), the band would be expected to be more pronounced at lower energy, and shift to higher energy as the polarity of the solvent decreases; this is opposite to what is actually observed. Insertion of the phenylene group between the Bodipy and quinone removes the severe absorption band broadening, and in fact the spectrum for **BD-SPQ** (Figure 3) is very similar to that for **BD-SPHQ**. Severe perturbation of the electronic transitions within the 2-substituted Bodipy derivatives is seen only for the quinone group attached directly at the 2-position. This is corroborated by spectroelectrochemical experiments performed on a solution of **BD-SQ** in CH_3CN

containing 0.2 M TBATFB in a standard OTTLE cell. Controlled coulombic reduction of the solution gives way to appearance of an absorption band that matches almost exactly with the hydroquinone derivative. Furthermore, the process is fully reversible since controlled oxidation of the solution affords the original spectrum. That the quinone unit in **BD-SQ** can rotate freely may have some bearing on the absorption spectrum profile. Unhindered rotation means that a wider envelope of geometries can be sampled, especially those which bring the Bodipy and quinone into partial conjugation. This is not so possible in the hydroquinone/benzyloxy versions because of steric constraints as discussed previously.

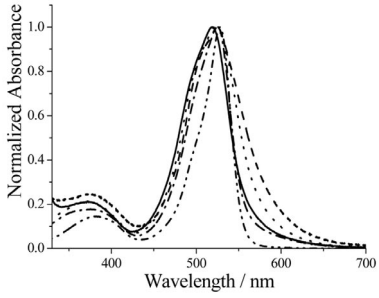

Figure 3. Normalized absorption spectra for **BD-SQ** in CH_3CN (–), toluene (– –), Me/THF (···), and formamide (–·–) and spectrum for **BD-SPQ** in CH_3CN (–··).

Femtosecond Time-Resolved Spectroscopy

Up-conversion fluorescence lifetime measurements carried out on **BD-SHQ** and **BD-MHQ** in CH_3CN affords decay profiles that cannot be fitted adequately to a single mono-exponential.[28] The fluorescence decay curve for **BD-SHQ** is best fitted as a tri-exponential τ_1 = 0.8 ps (32%), τ_2 = 3.4 ps (43%), τ_3 = 11.6 ps (25%). In comparison, the fluorescence decay for **BD-MHQ** is suitably fitted to a bi-exponential [τ_1 = 34 ps (35%), τ_2 = 273 ps (65%)], and there is no improvement to the fit by using a tri-exponential function (see Supporting Information).

Differential transient absorption records collected at four different time delays following excitation of **BD-SHQ** in CH_3CN with a 70 fs laser pulse delivered at 420 nm are illustrated in Figure 4. The transient absorption profile after 1.2 ps shows a clear bleach in the 565 nm region, which is associated with the ground-state S_0–S_1 electronic transition. A minor modification to the transient profile is seen over some 400 fs which is assigned to stimulated emission and/or is associated with relaxation of the S_1 state.[29] The transient absorption profiles over some 20 ps remain relatively constant in shape, and at long time delays (≈ 1 ns) there is no indication in the absorption records of a long-lived transient. Decay kinetics measured in the region associated with the strong bleach (526 nm) fit to a single exponential corresponding to a lifetime of 13 ps. A similar fit at 565 nm affords a decay lifetime of 2.5 ps. For both cases the decay curves return to the pre-pulse baseline, which is consistent with the lack of existence of a long-lived transient.

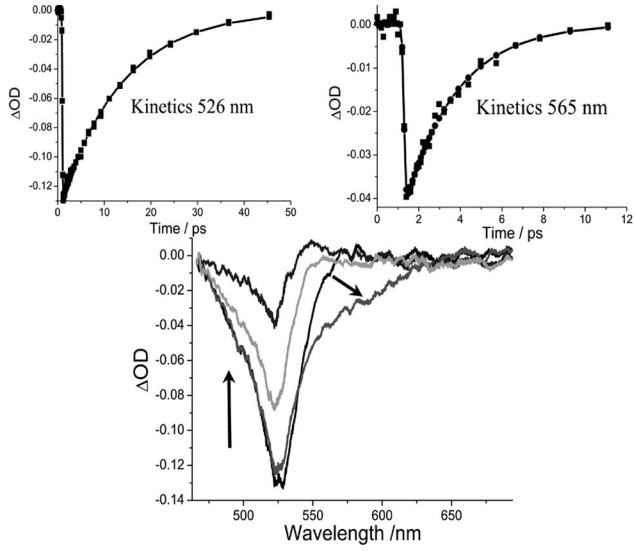

Figure 4. Differential transient absorption records measured at different time delays (1.2 ps, 1.6 ps, 7.8 ps, 19.7 ps) following excitation of **BD-SHQ** in CH_3CN with a 70 fs laser pulse delivered at 420 nm. Inserts show decay kinetics measured at two different wavelengths and the least-squares fit (solid line) to single exponential decays.

Differential transient absorption profiles collected for **BD-MHQ** in CH_3CN, following excitation with a 70 fs laser pulse (see Supporting Information), are overall similar in appearance to those shown in Figure 4. A strong bleach is seen at around 525 nm after 1.2 ps, which is accompanied by an increase in bleach to the lower-energy region at around 565 nm over 400 fs; this change is very similar to what is observed for **BD-SHQ**. Whereas the bleach at 525 nm continues to grow-in slightly over a further 20 ps or so, the change in optical density at 565 nm remains invariable over this time scale (see Supporting Information). Optical changes at 525 nm fit well to two exponentials corresponding to a grown-in over 23 ps and a slower decay of 289 ps. There is no sign of a long-lived transient in the spectral records.

Based on thermodynamic considerations (see Supporting Information) electron transfer from the hydroquinone to the excited Bodipy S_1 state for derivatives, **BD-MHQ** and **BD-SHQ**, is favourable. Despite this, the transient spectral records show no clear features at around 580 nm being attributable to the Bodipy-based radical anion.[30] From this it is inferred that either once formed the charge separated state (CSS) collapses back to the ground state by ultrafast charge recombination [despite the large exogenicity for the process ($\Delta G_{CR} \approx -2.2$ eV)], or an additional excited S_1 deactivation process associated with the hydroxy groups is introduced and the CSS is bypassed. Up-conversion fluorescence data for **BD-SHQ** is certainly consistent with fast processes evolving from the excited S_1 state; the 800 fs contribution is basically on a timescale in line with vibrational relaxation. The slower components (3.4 ps and 11.6 ps) from the up-conversion fluorescence experiments are similar to the two lifetimes (2.5 ps and 13 ps) as measured by transient

absorption spectroscopy. A basic model to explain these findings is the first lifetime represents the timescale required to create a suitable geometry, via structural alteration of the vibrationally cooled S_1 state, from which to facilitate electron transfer and produce the CSS. The second lifetime component symbolizes the timescale for charge separation, with charge recombination occurring with a rate constant (k_{CR}) greater than 8×10^{10} s^{-1}. That the structural change required to assist electron transfer within **BD-MHQ** is noticeably slower (cf. **BD-SHQ**), is at least consistent with the two compounds geometrical differences. The hydroquinone group in **BD-MHQ** is almost orthogonal to the Bodipy plane because of steric constraints imposed by the two flanking methyl groups; this restraint is more relaxed in **BD-SHQ**. A simple way to promote rapid electron transfer is to bring into partial π-conjugation the hydroquinone unit and the dipyrromethene of the Bodipy. For this to occur, especially for **BD-MHQ**, the two methyl groups must distort out of the Bodipy plane to allow the hydroquinone moiety to rotate more freely. High-level computational studies on excited-state structure dynamics for the two derivatives may be able to address this issue, but are beyond our calculation capabilities presently. This type of "gated" electron transfer[31] has been shown to operate in donor-bridge-acceptor molecules comprising a tetracene donor, pyromellitimide acceptor and oligo-*p*-phenylenevinylenes bridges.[32] For such assemblies the charge separation process is controlled by the torsional motion between the tetracene and the first phenyl group of the bridge. Very recent work by Vauthey et al. has also noted that charge separation dynamics in a Bodipy-dinitrotriptycene derivative are controlled by the reorientational motion of the donor relative to the acceptor.[29]

The one question that remains unanswered if our analysis is correct is why is charge recombination so fast? Generally, highly exogenic electron transfer as described above is associated with the so-called Marcus inverted region ($-\Delta G_{CR} > \lambda$), and one upshot is that CSS formation is generally faster than its decay.[33] The full effect of the Marcus inverted region can be obscured by secondary factors such as triplet formation,[34] quantum mechanical phenomenon[35] and nuclear tunneling,[36] however. Evidently, triplet formation at the Bodipy center can be ruled out, despite its known low-energy (ca. 12,800 cm^{-1}),[37] since time-resolved spectral records show no sign of a long-lived transient. High frequency vibrational modes play a critical role in return electron transfer in the inverted region, as seen for strongly interacting zinc(II)-porphyrin-imide dyads described by Osuka and co-workers.[38] The observed rate of charge recombination is in the order of 10^{11} s^{-1} for $-\Delta G_{CR} \approx 2$ eV, albeit in aprotic DMF, which is at least in the correct time-scale required to rationalize our results. An ideal candidate for the high-energy vibration that couples to return electron transfer is the OH stretching vibration ($\hbar\omega \approx 3500$ cm^{-1}, 0.43 eV) for the proximal hydroquinone group; two quanta being enough to reduce significantly the exergonicity for charge recombination.[39] Unfortunately, it is not practical at this stage to rule out possible contributions from proton-coupled electron transfer,[40] but more structure-sensitive ultrafast time-resolved spectroscopy (e.g., IR, Raman) is needed to really address this issue properly.

The excited state quenching of the Bodipy center for the quinone derivatives is subject to a separate publication[41] since solvent plays a very significant role and a more detailed analysis is required. In polar solvents time-resolved records are consistent with the formation of the Bodipy radical cation following photoinduced electron transfer from the first-excited singlet state to the adjacent quinone group. This is followed by rapid charge recombination. The behavior for the phenylene spacer derivatives in non-polar solvents is a little more complex requiring the need to invoke an exciplex as the quencher state.

Conclusions

A series of side-on Bodipy-based dyads have been successfully prepared incorporating either hydroquinone or quinone groups. The dyads represent the complement series to the previously published compounds where the *meso* position was the attachment site.[9] There are some noticeable differences in the properties of the compounds when the two series are compared, especially in their redox chemistry and photophysical properties. In particular, it is immediately apparent that the first-excited state deactivation by electron transfer for **BD-SHQ** is much faster (ca. 20 fold) when compared to the *meso* derivative **BD-MHQ**. Similar differences have been observed in energy transfer involving Bodipy-anthracene cassettes, where the substitution pattern is found to be crucial.[22] The excited state lifetime of the Bodipy is not dramatically improved by insertion of a phenylene group between the Bodipy and hydroquinone center for the 2-substituted derivative. In comparison, the change in lifetime for the *meso* compound is far more dramatic by addition of the phenylene unit. This work has demonstrated that the substitution position on the Bodipy group is critical, especially in the design of molecular probes where an on/off switching in fluorescence signal is paramount.

Experimental Section

Materials: Bulk chemicals were purchased as the highest purity possible from Aldrich Chemical Co. and used as received unless otherwise stated. Tetra-*n*-butylammonium tetrafluoroborate (TBATFB) purchased from Fluka was recrystallized several times from methanol and dried thoroughly under vacuum before being stored in a desiccator. Standard solvents were dried by literature methods before being distilled and stored under nitrogen over 4 Å molecular sieves. Spectroscopic grade solvents were used in all fast kinetic experiments and fluorescence/absorption spectroscopy measurements.

Instrumentation: ^1H and ^{13}C NMR spectra were recorded with either Bruker AVANCE 300 MHz, JEOL 400 MHz, or JEOL Lambda 500 MHz spectrometers. ^{11}B and ^{19}F NMR spectra were recorded using the 400 MHz spectrometer. Chemical shifts for ^1H and ^{13}C NMR spectra are referenced relative to the residual protiated solvent. The ^{11}B NMR chemical shift is referenced relative to

$BF_3{\cdot}Et_2O$ (δ = 0 ppm), and the ^{19}F NMR chemical shift is given relative to $CFCl_3$ (δ = 0 ppm). Routine mass spectra and elemental analyses were obtained using in-house facilities. MALDI mass spectra were recorded at the EPSRC-sponsored Mass Spectrometry Service at Swansea. Absorption spectra were recorded using a Hitachi U3310 spectrophotometer and corrected fluorescence spectra were recorded using a Lambda Advanced F 4500 spectrometer. Uncorrected melting points were measured using a Stuart SMP11 apparatus and typically carried out twice to check for consistency in the readings.

Cyclic voltammetry experiments were performed using a fully automated HCH Instruments Electrochemical Analyzer and a three-electrode set-up consisting of a platinum working electrode, a platinum wire counter electrode and a silver wire reference electrode. Ferrocene was used an internal standard. All studies were performed in deoxygenated CH_2Cl_2 containing TBATFB (0.2 M) as background electrolyte. The solute concentrations were typically 0.1 mM. Redox potentials were reproducible to within $\pm$15 mV. Spectroelectrochemistry experiments were performed in CH_2Cl_2 (TBATFB, 0.2 M) solutions and an Omini-cell specac OTTLE cell placed inside a Perkin–Elmer Lambda 35 UV/Vis spectrometer. In a typical experiment the working electrode was stepped to a fixed potential for several minutes and the absorption spectrum recorded. The reversibility of an electrochemical process was checked by carrying out the same procedure but with a potential set with an opposite sign. Several cycles were performed to check for compound degradation.

All luminescence measurements were made using optically dilute solutions and were corrected for spectral imperfections of the instrument by reference to a standard lamp. Luminescence quantum yields were measured relative to a standard Bodipy in acetonitrile using optically matched solutions and were measured twice for consistency in calculated values. Radiative rate constants were calculated from absorption and normalized fluorescence spectra using the Strickler–Berg equation[23] and compared to those calculated from lifetime and quantum yield measurements.

Synthesis: All preparations were carried out, unless otherwise stated, under a dry N_2 atmosphere in thoroughly oven-dried glassware.

Preparation of 1: To a stirred solution of 4-bromo-3,5-dimethyl-1*H*-pyrrole-2-carbaldehyde (1 g, 4.95 mmol, 1 equiv.) and 4-(dimethylamino)pyridine (200 mg) in THF (50 mL) at room temperature was added di-*tert*-butyl dicarbonate (1.4 g, 6.43 mmol, 1.3 equiv.) in a single portion. The reaction was heated to reflux until TLC showed complete consumption of the starting material. The THF was removed, and the residue was taken up into diethyl ether, washed with 1 M aqueous $NaHSO_4$ (3 × 100 mL), brine (3 × 100 mL), and saturated $NaHCO_3$ before being dried (Na_2SO_4). The solvent was removed under reduced pressure, yielding the crude product. The latter product was chromatographed on a silica gel (CH_2Cl_2/petroleum ether, 1:3), yielding the product as a pale brown solid (1.36 g, 91%); m.p. 82–84 °C. ^1H NMR ($CDCl_3$, 300 MHz): δ = 9.96 (s, 1 H), 2.45 (s, 3 H), 2.32 (s, 3 H), 1.61 (s, 9 H) ppm.

Preparation 2a: To a stirred solution of (2-bromo-1,4-phenylene)-bis(oxy)bis(methylene)dibenzene (1.8 g, 4.87 mmol, 1 equiv.) in THF (50 mL) at –78 °C was added dropwise *t*BuLi 1.7 M (4.01 mL, 6.82 mmol, 1.4 equiv.), immediately followed by addition of triethyl borate (2.48 mL, 14.6 mmol, 3 equiv.) dropwise at –78 °C. This temperature was maintained for 10 min, after which the solution was warmed to room temperature and stirred for 2 h. The reaction was cooled to 0 °C and quenched with a saturated solution of ammonium chloride (30 mL), followed by removal or the solvent under reduced pressure. Ethyl acetate was used to extract the product, before washing with water (100 mL) and brine (100 mL). The organic layer was then dried ($MgSO_4$) and the solvent was removed under reduced pressure, yielding the crude product which was chromatographed on silica gel (petroleum ether/ethyl acetate, 3:2). The final product was isolated as a white solid (1.3 g, 83%); m.p. 113–115 °C. ^1H NMR ($CDCl_3$, 300 MHz): δ = 7.55 (d, J = 3.1 Hz, 1 H), 7.39 (m, 10 H), 7.05 (dd, J = 8.9, J' = 3.1 Hz, 1 H), 6.92 (d, J = 8.9 Hz, 1 H), 6.49 (br. s, 2 H), 5.10 (s, 2 H), 5.06 (s, 2 H) ppm. ^{13}C NMR ($CDCl_3$, 75 MHz): δ = 158.82, 153.89, 137.81, 136.73, 129.24, 128.83, 128.16, 128.05, 127.83, 122.95, 120.06, 113.33, 71.99, 71.26 ppm. IR (neat): $\tilde{\nu}$ = 3494, 3389 (O–H), 2875 (C–H) cm^{-1}.

Preparation of 2,5-Bis(benzyloxy)-4′-bromobiphenyl: To a stirred solution of 2-(4-bromophenyl)cyclohexa-2,5-diene-1,4-diol (1.55 g, 5.85 mmol, 1 equiv.), K_2CO_3 (1.13 g, 8.19 mmol, 1.4 equiv.) in acetone (25 mL) was added benzyl bromide (1.67 mL, 14 mmol, 2.4 equiv.). The mixture was heated at reflux until TLC showed complete consumption of the starting material. At this point, the reaction was allowed to cool and the K_2CO_3 was removed via filtration. The solvent was removed under reduced pressure, yielding the crude product which was chromatographed on silica gel (petroleum ether/CH_2Cl_2, 3:1) affording a white solid (2.39 g, 92%); m.p. 96–98 °C. ^1H NMR ($CDCl_3$, 300 MHz): δ = 7.31 (m, 14 H), 6.882 (m, 2 H), 6.81 (dd, J = 8.8, J' = 2.9 Hz, 1 H), 4.96 (s, 2 H), 4.89 (s, 2 H) ppm. ^{13}C NMR ($CDCl_3$, 75 MHz): δ = 154.11, 150.58, 137.75, 137.70, 137.65, 132.07, 131.53, 131.42, 128.86, 128.72, 128.22, 128.02, 127.76, 127.49, 121.60, 118.14, 116.26, 115.39, 72.41, 71.37 ppm. EI-MS: *m*/*z* calcd. for $C_{26}H_{21}BrO_2$ (445), found 445. $C_{26}H_{21}BrO_2$ (445): calcd. C 70.12, H 4.75; found C 70.19, H 4.67.

Preparation of 2b: To a stirred solution of 2,5-bis(benzyloxy)-4′-bromobiphenyl (2.1 g, 4.72 mmol, 1 equiv.) in THF (100 mL) at –78 °C was added *t*BuLi 1.7 M (3.88 mL, 6.6 mmol, 1.4 equiv.) dropwise, immediately followed by the dropwise addition of triethylborate (2.41 mL, 14 mmol, 3 equiv.) at –78 °C. This temperature was maintained for 10 min, after which the solution was warmed to room temperature before being stirred for a further 2 h. The reaction was cooled to 0 °C and quenched with a saturated solution of ammonium chloride (30 mL), followed by removal of the reaction solvent under reduced pressure. Ethyl acetate was used to extract the product. The organic phase was washed with water (100 mL) and brine (100 mL). The organic layer was then dried ($MgSO_4$), and the solvent was removed under reduced pressure, yielding the crude product. This latter material was chromatographed on silica gel (petroleum ether/ethyl acetate, 1:1) to afford the product as a white solid (1.64 g, 85%); m.p. 70–72 °C. ^1H NMR ($CDCl_3$, 300 MHz): δ = 8.24 (d, J = 8 Hz, 2 H), 7.66 (d, J = 8 Hz, 2 H), 7.24 (m, 10 H), 7.01 (d, J = 2.9 Hz, 1 H), 6.92 (d, J = 8.9 Hz, 1 H), 6.85 (dd, J = 8.9, J' = 2.9 Hz, 1 H), 5.00 (s, 2 H), 4.94 (s, 2 H) ppm. ^{13}C NMR ($CDCl_3$, 75 MHz): δ = 154.14, 150.81, 143.26, 137.82, 137.78, 135.70, 133.19, 129.54, 128.87, 128.71, 128.20, 127.94, 127.80, 127.50, 118.37, 116.48, 116.45, 115.51 ppm (note: two carbon resonances missing due to accidental equivalence). EI-MS: *m*/*z* calcd. for $C_{26}H_{23}BO_4$ (410), found 410. $C_{26}H_{23}BO_4$ (410): calcd. C 76.12, H 5.65; found C 76.18, H 5.59.

Preparation of 3a: Compound **1** (1 g, 3.3 mmol, 1 equiv.), and **2a** (2.2 g, 6.6 mmol, 2 equiv.) were dissolved in DMF (100 mL), and the resultant solution was purged with nitrogen for 1 h. To this solution was added a nitrogen-purged aqueous solution of 2 M Na_2CO_3 (6.6 mL, 13.2 mmol, 4 equiv.), followed by $Pd(PPh_3)_4$

(0.38 g, 10 mol-%). The reaction mixture was refluxed overnight. The resulting reaction mixture was allowed to cool to room temperature, and the product was extracted into CH_2Cl_2 (3 × 100 mL). The organic layer was washed with brine (3 × 50 mL) and dried ($MgSO_4$). The solvent was removed under reduced pressure, to yield a dark brown residue. This material was chromatographed on silica gel (ethyl acetate/petroleum ether, 1:1), yielding a light brown solid (1.01 g, 75% yield); m.p. 148–150 °C. ^{1}H NMR (300 MHz, $CDCl_3$): δ = 10.26 (br. s, 1 H), 9.43 (s, 1 H), 7.00 (m, 10 H), 6.87 (d, J = 8.8 Hz, 1 H), 6.80 (dd, J = 8.8, J' = 2.8 Hz, 1 H), 6.68 (d, J = 2.8 Hz, 1 H), 4.94 (s, 2 H), 4.82 (s, 2 H), 2.08 (s, 6 H) ppm. ^{13}C NMR (75 MHz, $CDCl_3$): δ = 176.52, 153.75, 151.81, 137.83, 136.85, 128.88, 128.69, 128.19, 127.97, 127.75, 127.46, 125.82, 122.25, 119.62, 116.44, 115.32, 72.53, 71.31, 12.62, 9.75 ppm. EI-MS: *m*/*z* calcd. for $C_{27}H_{25}NO_3$ (411), found 411. $C_{27}H_{25}NO_3$ (411): C 78.81, H 6.12 (6.19), N 3.40 (3.30).

Preparation of 3b: The same procedure are described above was used. Compound **1** (0.4 g, 1.3 mmol, 1 equiv.), **2b** (1.08 g, 2.63 mmol, 2 equiv.), DMF (80 mL), 2 M Na_2CO_3 (5.5 mL, 11 mmol, 4 equiv.) and $Pd(PPh_3)_4$ (0.15 g, 10 mol-%). Purification: silica gel, ethyl acetate/petroleum ether (1:2). Brown solid (0.43 g, 67%); m.p. 172–174 °C. ^{1}H NMR (300 MHz, $CDCl_3$): δ = 9.61 (br. s, 1 H), 9.52 (s, 1 H), 7.56 (d, J = 8.2 Hz, 2 H), 7.28 (m, 12 H), 7.01 (d, J = 2.9 Hz, 1 H), 6.915 (d, J = 8.9 Hz, 1 H), 6.83 (dd, J = 8.9, J' = 2.9 Hz, 1 H), 4.99 (s, 2 H), 4.93 (s, 2 H), 2.29 (s, 3 H), 2.28 (s, 3 H) ppm. ^{13}C NMR (75 MHz, $CDCl_3$): δ = 176.77, 154.21, 150.86, 137.91, 137.13, 133.29, 133.17, 129.92, 129.72, 128.84, 128.61, 128.17, 127.90, 127.77, 127.47, 118.23, 116.50, 115.12, 72.55, 71.37, 12.57, 9.66 ppm. EI-MS: *m*/*z* calcd. for $C_{33}H_{29}NO_3$ (487), found 487. $C_{33}H_{29}NO_3$ (487): calcd. C 81.29, H 5.99, N 2.87; found C 81.17, H 6.01, N 2.80.

Preparation of BD-SPBn: To a stirred solution of 3-ethyl-2,4-dimethylpyrrole (0.16 mL, 1.2 mmol, 1 equiv.) and **3b** (0.5 g, 1.2 mmol, 1 equiv.) in CH_2Cl_2 (100 mL) was added TFA (2 drops). The reaction was allowed to stir at room temperature until TLC showed complete consumption of the aldehyde. *N*,*N*-Diisopropylethylamine (1.164 mL, 6.9 mmol, 5.7 equiv.) and $BF_3{\cdot}Et_2O$ (1.24 mL, 9.7 mmol, 8 equiv.) were added and the reaction was left to stir for 6 h at room temperature. The mixture was washed with water (3 × 100 mL) and brine (3 × 100 mL). The separated organic fractions were dried ($MgSO_4$), filtered and evaporated to yield a black/dark violet residue with a green tint. The residue was chromatographed on silica gel (toluene), yielding the product as a bright red solid (0.33 g, 42% yield); m.p. 199–201 °C. ^{1}H NMR ($CDCl_3$, 300 MHz): δ = 7.55 (d, J = 8.2 Hz, 2 H), 7.26 (m, 12 H), 7.00 (m, 2 H), 6.90 (d, J = 8.9 Hz, 1 H), 6.81 (dd, J = 8.9, J' = 2.9 Hz, 1 H), 4.98 (s, 2 H), 4.91 (s, 2 H), 2.49 (s, 3 H), 2.46 (s, 3 H), 2.32 (q, J = 7.5 Hz, 2 H), 2.17 (s, 3 H), 2.11 (s, 3 H), 1.00 (t, J = 7.5 Hz, 3 H) ppm. ^{13}C NMR ($CDCl_3$, 75 MHz): δ = 157.18, 154.19, 153.98, 150.85, 137.89, 137.82, 137.41, 136.53, 133.80, 133.14, 133.09, 132.93, 132.78, 131.64, 129.94, 129.64, 128.87, 128.65, 128.20, 127.95, 127.80, 127.48, 119.62, 118.16, 116.48, 115.16, 72.54, 71.34, 17.66, 14.65, 13.63, 12.99, 10.46, 9.65 ppm. IR (neat): $\tilde{\nu}$ = 2960 (C–H), 1599, 1453 (C=C, C=N), 1189 (B–F) cm^{-1}. EI-MS: *m*/*z* calcd. for $C_{41}H_{39}BF_2N_2O_2$ (640), found 640. $C_{41}H_{39}BF_2N_2O_2$ (640): calcd. C 76.88, H 6.14, N 4.37; found C 76.82, H 6.17, N 4.31.

Preparation of BD-SBn: The same procedure as described above was used. 3-Ethyl-2,4-dimethylpyrrole (0.49 mL, 3.6 mmol, 1 equiv.), **3a** (1.37 g, 3.3 mmol, 1 equiv.), CH_2Cl_2 (250 mL), TFA (2 drops), *N*,*N*-diisopropylethylamine (3.18 mL, 19 mmol, 5.7 equiv.) and $BF_3{\cdot}Et_2O$ (3.78 mL, 26 mmol, 8 equiv.). Purification: silica gel, toluene eluant. Bright red solid (0.82 g, 44%); m.p. 128–130 °C. ^{1}H NMR ($CDCl_3$, 300 MHz): δ = 7.23 (m, 10 H), 6.81 (m, 3 H), 6.67 (s, 1 H), 4.94 (s, 2 H), 4.84 (s, 2 H), 2.44 (s, 3 H), 2.30 (m, 5 H), 2.09 (s, 3 H), 1.98 (s, 3 H), 1.04 (t, J = 7.5 Hz, 3 H) ppm. ^{13}C NMR ($CDCl_3$, 75 MHz): δ = 156.28, 155.35, 153.73, 151.67, 138.25, 137.77, 137.42, 133.43, 132.88, 132.54, 128.85, 128.74, 128.57, 128.17, 127.94, 127.73, 127.50, 127.52, 119.51, 119.16, 116.45, 115.75, 72.53, 71.33, 17.64, 14.66, 13.69, 12.90, 10.51, 9.59 ppm (note: one carbon resonance is missing due to accidental equivalence). ^{11}B NMR ($CDCl_3$, 160 MHz): δ (ppm) = –0.00 (t, J_{av} = 33.09 Hz). ^{19}F NMR ($CDCl_3$, 470 MHz): δ = –146.3 (m) ppm. IR (neat): $\tilde{\nu}$ = 2960 (C–H), 1598, 1496 (C=C, C=N), 1186 (B–F) cm^{-1}. EI-MS: *m*/*z* calcd. for $C_{35}H_{35}BF_2N_2O_2$ (564), found 564. $C_{35}H_{35}BF_2N_2O_2$ (564): calcd. C 74.47, H 6.25, N 4.96; found C 74.28, H 6.22, N 4.92.

Preparation of BD-SHQ: To a thoroughly degassed solution of **BD-SBn** (0.3 g, 0.51 mmol, 1 equiv.) and 1,4-cyclohexadiene (1.98 mL, 21 mmol, 40 equiv.) in ethanol was added $Pd(OH)_2$/C (50 mg). The reaction was refluxed until TLC showed complete consumption of the starting material. The mixture was filtered through a pad of celite and concentrated under vacuum. The residue was chromatographed on silica gel (chloroform), yielding the final product as a red solid (0.2 g, 93%); m.p. 134–136 °C. ^{1}H NMR ($CDCl_3$, 300 MHz): δ = 7.06 (s, 1 H), 6.78 (d, J = 8.6 Hz, 1 H), 6.73 (dd, J = 8.6, J' = 2.6 Hz, 1 H), 6.53 (d, J = 2.6 Hz, 1 H), 5.06 (br. s, 1 H), 4.76 (br. s, 1 H), 2.54 (s, 3 H), 2.44 (m, 5 H), 2.19 (s, 3 H), 2.09 (s, 3 H), 1.08 (t, J = 7.5 Hz, 3 H) ppm. ^{13}C NMR ($CDCl_3$, 75 MHz): δ = 159.16, 153.35, 149.54, 148.25, 138.95, 137.85, 134.41, 133.76, 132.48, 124.94, 121.03, 119.76, 117.98, 116.81, 116.54, 17.61, 14.47, 13.12, 13.11, 10.18, 9.61 ppm. ^{11}B NMR ($CDCl_3$, 160 MHz): δ = –0.00 (t, J_{av} = 34.4 Hz) ppm. ^{19}F NMR ($CDCl_3$, 470 MHz): δ = –145.63 (m, 2 F) ppm. IR (neat): $\tilde{\nu}$ = 3497 (OH), 2965 (C–H), 1598, 1462 (C=C, C=N), 1186 (B–F) cm^{-1}. EI-MS: *m*/*z* calcd. for $C_{21}H_{23}BF_2N_2O_2$ (384), found 384. $C_{21}H_{23}BF_2N_2O_2$ (384): calcd. C 65.65, H 6.03, N 7.29; found C 65.59, H 6.14, N 7.17.

Preparation of BD-SPHQ: The same procedure to above was used. **BD-SPBn** (0.36 g, 0.56 mmol, 1 equiv.), 1,4-cyclohexadiene (2.11 mL, 22 mmol, 40 equiv.), ethanol (50 mL), $Pd(OH)_2$/C (50 mg). Purification: silica gel, petroleum ether/ethyl acetate (1:1) eluant. Red solid (0.25 g, 98%); m.p. 150–152 °C. ^{1}H NMR (MeOD, 300 MHz): δ = 7.59 (d, J = 8.2 Hz, 2 H), 7.20 (m, 3 H), 6.73 (m, 3 H), 2.47 (s, 3 H), 2.46 (s, 3 H), 2.33 (q, J = 7.5 Hz, 2 H), 2.10 (s, 3 H), 2.08 (s, 3 H), 1.01 (t, J = 7.5 Hz, 3 H) ppm. ^{13}C NMR (MeOD, 75 MHz): δ = 158.08, 154.46, 152.03, 148.78, 140.05, 139.32, 138.40, 135.20, 135.18, 134.24, 134.08, 133.98, 132.72, 130.89, 130.80, 121.54, 118.65, 118.47, 116.73, 18.47, 15.15, 14.00, 13.30, 10.67, 9.83 ppm. ^{11}B NMR (MeOD, 160 MHz): δ (ppm) = –0.057 (t, J_{av} = 31.99 Hz). ^{19}F NMR (MeOD, 470 MHz): δ = –145.550 (q, J_{av} = 28.15 Hz) ppm. IR (neat): $\tilde{\nu}$ = 3525 (OH), 2967 (C–H), 1539, 1455 (C=C, C=N), 1184 (B–F) cm^{-1}. EI-MS: *m*/*z* calcd. for $C_{27}H_{27}BF_2N_2O_2$ (460), found 460. $C_{27}H_{27}BF_2N_2O_2$ (460): calcd. C 70.45, H 5.91, N 6.09; found C 70.54, H 5.90, N 6.00.

Preparation of BD-SQ: To a stirred solution of the **BD-SHQ** (0.9 g, 2.34 mmol, 1 equiv.) in THF (50 mL) was added DDQ (0.79 g, 3.51 mmol, 1.5 equiv.). On addition of the DDQ, the reaction mixture changed from red to dark purple. When TLC showed complete consumption of the starting material, the solvent was removed and the residue was taken into CH_2Cl_2 (100 mL) and washed with water (3 × 100 mL). The combined organic fractions were dried ($MgSO_4$). The residue was chromatographed on silica gel (petroleum ether/chloroform, 1:1), yielding the crude product as a purple solid

(0.89 g, 94%); m.p. 178–180 °C. ^{1}H NMR ($CDCl_3$, 300 MHz): δ = 7.06 (s, 1 H), 6.82 (m, 2 H), 6.62 (d, J = 1.9 Hz, 1 H), 2.53 (s, 3 H), 2.38 (m, 5 H), 2.18 (s, 3 H), 2.12 (s, 3 H), 1.07 (t, J = 7.5 Hz, 3 H) ppm. ^{13}C NMR ($CDCl_3$, 75 MHz): δ (ppm) = 187.49, 186.19, 160.60, 152.70, 142.00, 139.50, 137.26, 136.72, 135.02, 134.91, 134.41, 132.29, 122.28, 120.00, 17.61, 14.39, 13.74, 13.19, 10.79, 9.60. ^{11}B NMR ($CDCl_3$, 160 MHz): δ (ppm) = –0.10 (t, J_{av} = 33.09 Hz). ^{19}F NMR ($CDCl_3$, 470 MHz): δ (ppm) = –145.83 (q, J_{av} = 32.73 Hz). IR (neat): $\tilde{\nu}$ = 2961 (C–H), 1661 (C=O), 1532, 1444 (C=C, C=N), 1187 (B–F) cm^{-1}. EI-MS: *m*/*z* calcd. for $C_{21}H_{21}BF_2N_2O_2$ (382), found 382. $C_{21}H_{21}BF_2N_2O_2$ (382): calcd. C 65.99, H 5.54, N 7.33; found C 65.93, H 5.68, N 7.32.

Preparation of BD-SPQ: The same procedure to above was used. **BD-SPHQ** (0.23 g, 0.49 mmol, 1 equiv.), THF (50 mL), DDQ (0.17 g, 0.74 mmol, 1.5 equiv.). Purification: silica gel, petroleum ether/chloroform (1:1) eluant. Purple solid (0.22 g, 97%); m.p. 217–219 °C. ^{1}H NMR ($CDCl_3$, 300 MHz): δ = 7.53 (d, J = 8.2 Hz, 2 H), 7.31 (d, J = 8.2 Hz, 2 H), 7.06 (s, 1 H), 6.89 (d, J = 2.3 Hz, 1 H), 6.86 (d, J = 10.1 Hz, 1 H), 6.81 (dd, J = 10.1, J' = 2.3 Hz, 1 H), 2.52 (s, 6 H), 2.38 (q, J = 7.5 Hz, 2 H), 2.20 (s, 3 H), 2.17 (s, 3 H), 1.06 (t, J = 7.5 Hz, 3 H) ppm. ^{13}C NMR ($CDCl_3$, 75 MHz): δ = 187.63, 187.84, 158.00, 152.48, 145.53, 138.34, 137.14, 136.38, 136.32, 135.92, 133.77, 133.12, 132.42, 132.09, 131.05, 129.89, 129.41, 17.39, 14.53, 13.41, 12.92, 10.36, 9.53 ppm. ^{11}B NMR ($CDCl_3$, 160 MHz): δ (ppm) = –0.00 (t, J_{av} = 33.21 Hz). ^{19}F NMR ($CDCl_3$, 470 MHz): δ = –146.04 (q, J_{av} = 32.81 Hz) ppm. IR (neat): $\tilde{\nu}$ = 2970 (C–H), 1652 (C=O), 1535, 1456 (C=C, C=N), 1184 (B–F) cm^{-1}. EI-MS: *m*/*z* calcd. for $C_{27}H_{25}BF_2N_2O_2$ (458), found 458. $C_{27}H_{25}BF_2N_2O_2$ (458): calcd. C 70.76, H 5.50, N 6.11; found C 70.81, H 5.44, N 6.09.

Supporting Information (see also the footnote on the first page of this article): Calculated thermodynamic parameters, Table of absorption/fluorescence data, simulated NMR spectra, electrochemistry, Beer–Lambert plot and additional fast kinetic data.

Acknowledgments

We thank the Engineering and Physical Sciences Research Council (EPSRC) and Newcastle University for financial support and the EPSRC sponsored National Mass Spectrometry Service at Swansea for obtaining mass spectra. We also thank Dr Bruce Tattershall and Prof William McFarlane for help in collecting NMR spectra and the fitting of the ^{19}F NMR spectroscopic data.

[1] For comprehensive reviews see: a) A. Loudet, K. Burgess, *Chem. Rev.* **2007**, *107*, 4891–4932; b) T. E. Wood, A. Thompson, *Chem. Rev.* **2007**, *107*, 1831–1861; c) G. Ulrich, R. Ziessel, A. Harriman, *Angew. Chem. Int. Ed.* **2008**, *47*, 1184–1201; d) R. Ziessel, G. Ulrich, A. Harriman, *New J. Chem.* **2007**, *31*, 496–501; e) K. Burgess, L. Wu, *Chem. Commun.* **2008**, 4933–4935; f) M. Shah, K. Thangraj, M. L. Soong, L. Wolford, J. H. Boyer, I. R. Poliitzer, T. G. Pavlopoulos, *Heteroat. Chem.* **1990**, *1*, 389–399; g) A. Burghart, H. Kim, M. B. Welch, L. H. Thoresnsen, J. Reibenspies, K. Burgess, *J. Org. Chem.* **1999**, *64*, 7813–7819.

[2] For a selection of examples see: a) M. D. Yilmaz, A. Bozdemir, E. U. Akkaya, *Org. Lett.* **2006**, *8*, 2871–2873; b) H. Y. Lee, D. R. Bae, J. C. Park, H. Song, W. S. Han, J. H. Jung, *Angew. Chem. Int. Ed.* **2009**, *48*, 1239–1243; c) K. Umezawa, A. Matsui, Y. Nakmura, D. Citterio, K. Suzuki, *Chem. Eur. J.* **2009**, *15*, 1096–1106; d) K. Rurack, M. Kollmannsberger, J. Daub, *Angew. Chem. Int. Ed.* **2001**, *40*, 385–387; e) M. M. Sartin, F. Camerel, R. Ziessel, A. J. Bard, *J. Phys. Chem. C* **2008**, *112*, 10833–10841; f) R. Guliyez, O. Buyukcakir, F. Sozman, O. A. Bozdemir, *Tetrahedron Lett.* **2009**, *50*, 5139–5141.

[3] A. C. Benniston, G. Copley, *Phys. Chem. Chem. Phys.* **2009**, *11*, 4124–4131.

[4] a) W. Qin, M. Baruah, W. M De Borggraeve, N. Boens, *J. Photochem. Photobiol.* **2006**, *183*, 190–197; b) C. N. Baki, E. U. Akkaya, *J. Org. Chem.* **2005**, *70*, 4152–4157.

[5] a) D. P. Kennedy, C. M. Kormos, S. C. Burdette, *J. Am. Chem. Soc.* **2009**, *131*, 8578–8586; b) X. Zhang, H.-S. Zhang, *Spec. Chim. Acta* **2005**, *61*, 1045–1049; c) T. Matsumoto, Y. Urano, T. Shoda, H. Kojima, T. Nagano, *Org. Lett.* **2007**, *9*, 3375–3377; d) X. Peng, J. Du, J. Fan, J. Wang, Y. Wu, J. Zhao, S. Sun, T. J. Xu, *J. Am. Chem. Soc.* **2007**, *129*, 1500–1501; e) A. Coskun, M. D. Yilmaz, E. U. Akkaya, *Org. Lett.* **2007**, *9*, 607–609; f) M. Baruah, W. Qin, R. A. L. Vallée, D. Beljonne, T. Rohand, W. Dehaen, N. Boens, *Org. Lett.* **2005**, *7*, 4377–4380; g) J.-P. Malval, I. Leray, B. Valeur, *New J. Chem.* **2005**, *29*, 1089–1094.

[6] R. Ziessel, G. Ulrich, A. Harriman, M. A. H. Alamiry, B. Stewart, P. Retailleau, *Chem. Eur. J.* **2009**, *15*, 1359–1369.

[7] a) Z.-N. Sun, F.-Q. Liu, Y. Chen, P. K. H. Tam, D. Yang, *Org. Lett.* **2008**, *10*, 2171–2174; b) Y. Yamada, Y. Tomiyama, A. Morita, M. Ikekita, S. Aoki, *ChemBioChem* **2008**, *9*, 853–856.

[8] A. Gomes, E. Fernades, J. L. F. C. Lima, *J. Biochem. Biophys. Methods* **2005**, *65*, 45–80.

[9] A. C. Benniston, G. Copley, K. J. Elliott, R. W. Harrington, W. Clegg, *Eur. J. Org. Chem.* **2008**, 2705–2713.

[10] a) Z. Dost, S. Atilgan, E. U. Akkaya, *Tetrahedron* **2006**, *62*, 8484–8488; b) D. Zhang, Y. Wen, Y. Xiao, G. Yu, Y. Liu, X. X. Qian, *Chem. Commun.* **2008**, 4777–4779.

[11] a) J. L. Sessler, M. R. Johnson, S. E. Creager, J. C. Fettinger, J. A. Ibers, *J. Am. Chem. Soc.* **1990**, *112*, 9310–9329; b) J. L. Sessler, V. L. Capuano, A. Harriman, *J. Am. Chem. Soc.* **1993**, *115*, 4618–4628.

[12] H. D. Tabb, K. M. Smith, *J. Org. Chem.* **1984**, *49*, 1870–1875.

[13] G. B. Marini-Bettolo, O. A. Polla, J. H. Abril, *Gazz. Chim. Ital.* **1950**, *80*, 76–84.

[14] N. Miyaura, K. Yamada, A. Suzuki, *Tetrahedron Lett.* **1979**, *36*, 3437–3440.

[15] The molecular structures can be viewed at the website http://www.ncl.ac.uk/mpl/, or alternatively they are presented in G. Copley, PhD Thesis, Newcastle University, **2009**.

[16] M. Bröring, R. Krüger, S. Link, C. Kleeberg, S. Köhler, X. Xie, B. Ventura, L. Flamigni, *Chem. Eur. J.* **2008**, *14*, 2976–2983.

[17] Molar volumes were calculated using data taken from: A. Bondi, *J. Phys. Chem.* **1964**, *68*, 441–451.

[18] T. R. Kelly, M. C. Bowyer, K. V. Bhaskar, D. Bebbington, A. Garcia, F. Lang, M. H. Kim, M. P. Jette, *J. Am. Chem. Soc.* **1994**, *116*, 3657–3658.

[19] In order to isolate the diastereoisomers no rotation of the appended group can take place in solution at ambient temperature. Very hindered rotation would be more probable using a large bulky chiral hydroxy protecting group starting from, for example, 1-bromomethyl-(+)-cuparene.

[20] a) Y. Zhou, Y. Xiao, D. Li, M. Fu, X. Qian, *J. Org. Chem.* **2008**, *73*, 1571–1574; b) J. Chen, A. Burghart, A. Derecskei-Kovacs, K. Burgess, *J. Org. Chem.* **2000**, *65*, 2900–2906.

[21] a) J. Bañuelos, F. L. Arbeloa, V. M. Martínez, T. A. López, I. L. Arbeloa, *Phys. Chem. Chem. Phys.* **2004**, *6*, 4247–4253; b) J. B. Prieto, F. L. Arbeloa, V. M. Martínez, I. L. Arbeloa, *Chem. Phys.* **2004**, *296*, 13–22.

[22] C.-W. Wan, A. Burghart, J. Chen, F. Bergström, L. B.-Å. Johansson, M. F. Wolford, T. G. Kim, M. R. Topp, R. M. Hochstrasser, K. Burgess, *Chem. Eur. J.* **2003**, *9*, 4430–4441.

[23] S. J. Strickler, R. A. Berg, *J. Chem. Phys.* **1962**, *37*, 814–822.

[24] J. H. Boyer, A. M. Haag, G. Sathyamoorthi, M.-L. Soong, K. Thangaraj, T. G. Pavlopoulos, *Heteroat. Chem.* **1993**, *4*, 39–49.

[25] R. Englman, J. Jortner, *Mol. Phys.* **1970**, *18*, 145–164.

[26] F. Bergström, I. Mikhalyov, R. Hägglöf, R. Wortmann, T. Ny, L. B.-Å. Johansson, *J. Am. Chem. Soc.* **2002**, *124*, 196–204.

[27] a) T. Rohand, J. Lycoops, S. Smout, E. Braeken, M. Sliwa, M. Van der Auweraer, W. Dehaen, W. M. De Borggraeve, N. Boens, *Photochem. Photobiol. Sci.* **2007**, *6*, 1061–1066; b) W. Qin, T. Rohand, M. Baruah, A. Stefan, M. Van der Auweraer, W. Dehaen, N. Boens, *Chem. Phys. Lett.* **2006**, *420*, 562–568; c) W. Qin, M. Baruah, M. Van der Auweraer, F. C. De Schryver, N. Boens, *J. Phys. Chem. A* **2005**, *109*, 7371–7384; d) W. Qin, M. Baruah, A. Stefan, M. Van der Auweraer, N. Boens, *ChemPhysChem* **2005**, *6*, 2343–2351.

[28] A single mono-exponential decay is not always observed and is often associated with other processes stemming from the excited-state such as vibrational cooling, proton transfer etc., see for example: H. Wang, H. Zhang, O. K. Abou-Zied, C. Yu, F. E. Romesberg, M. Glasbeek, *Chem. Phys. Lett.* **2003**, *367*, 599–608.

[29] G. Duvanel, N. Banerji, E. Vauthey, *J. Phys. Chem. A* **2007**, *111*, 5361–5369.

[30] S. Hattori, K. Ohkubo, Y. Urano, H. Sunhara, T. Nagano, Y. Wada, N. V. Tkachenko, H. Lemmetyinen, S. Fukuzumi, *J. Phys. Chem. B* **2005**, *109*, 15368–15375.

[31] a) P. P. Lainé, F. Bedioui, F. Loiseau, C. Chiorboli, S. Campagna, *J. Am. Chem. Soc.* **2006**, *128*, 7510–7521; b) K. Nomoto, S. Kume, H. Nishihara, *J. Am. Chem. Soc.* **2009**, *131*, 3830–3831.

[32] W. B. Davis, M. A. Ratner, M. R. Wasielewski, *J. Am. Chem. Soc.* **2001**, *123*, 7877–7886.

[33] R. A. Marcus, *Discuss. Faraday Soc.* **1960**, *29*, 21–31.

[34] a) P. L. Dutton, J. S. Leight, M. Seibert, *Biochem. Biophys. Res. Commun.* **1972**, *46*, 406–413; b) M. C. Thuranauer, J. J. Katz, J. R. Norris, *Proc. Natl. Acad. Sci. USA* **1975**, *72*, 3270–3274; c) K. Hasharoni, H. Levanon, S. R. Greenfield, D. J. Gosztola, W. A. Svec, M. R. Wasielewski, *J. Am. Chem. Soc.* **1995**, *117*, 8055–8056; d) M. R. Wasielewski, D. W. Minsek, M. P. Niemczyk, W. A. Svec, N. C. Yang, *J. Am. Chem. Soc.* **1990**, *112*, 2823–2824; e) J. Hu, B. Xia, D. Bao, A. Ferreira, J. Wan, G. Jones II, V. I. Vullev, *J. Phys. Chem. A* **2009**, *113*, 3096–3107.

[35] a) M. Bixon, J. Jortner, *Adv. Chem. Phys.* **1999**, *106*, 35–208; b) J. Kroon, H. Oevering, J. W. Verhoeven, J. M. Warman, A. M. Oliver, M. N. Paddon-Row, *J. Phys. Chem.* **1993**, *97*, 5065–5069; c) K. J. Smit, J. M. Warman, M. P. de Haas, M. N. Paddon-Row, A. M. Oliver, *Chem. Phys. Lett.* **1988**, *152*, 177–182; d) N. Liang, J. R. Miller, G. L. Closs, *J. Am. Chem. Soc.* **1990**, *112*, 5353–5354.

[36] a) S. Franzen, J. Martin, *Annu. Rev. Phys. Chem.* **1995**, *46*, 453–487; b) A. C. Benniston, G. M. Chapman, A. Harriman, M. Mehrabi, *J. Phys. Chem. A* **2004**, *108*, 9026–9036.

[37] A. A. Gorman, I. Hamblett, T. A. King, M. D. Rahn, *J. Photochem. Photobiol. A: Chem.* **2000**, *130*, 127–132.

[38] N. Yoshida, T. Ishizuka, K. Yofu, M. Murakami, H. Miyasaka, T. Okada, Y. Nagata, A. Itaya, H. S. Cho, D. Kim, A. Osuka, *Chem. Eur. J.* **2003**, *9*, 2854–2866.

[39] It also possible to explain the increase in the rate constant for charge recombination in terms of the energy gap law (see ref. 25). Generally, $\hbar\omega$ is taken to be around 1500 cm^{-1} when considering return electron transfer in donor-acceptor systems; the increase in $\hbar\omega$ to ca. 3500 cm^{-1} will concomitantly increase k_{NR} assuming all other parameters remain constant. This argument has been used to explain the rapid non-radiative deactivation of a charge-transfer state in a N–H-containing Bodipy-based tripartite array, see: M. A. H. Alamiry, A. Harriman, L. J. Mallon, G. Ulrich, R. Ziessel, *Eur. J. Org. Chem.* **2008**, 2774–2782.

[40] R. I. Cukier, D. G. Nocera, *Annu. Rev. Chem.* **1998**, *49*, 337–369.

[41] A. C. Benniston, G. Copley, H. Lemmetyinen, N. V. Tkachenko, *ChemPhysChem* **2010**, in press.

Received: February 17, 2010
Published Online: April 14, 2010

